Bitcoin Price Regime Shifts: A Bayesian MCMC and Hidden Markov Model Analysis of Macroeconomic Influence

Vaiva Pakštaitė, Ernestas Filatovas *, Mindaugas Juodis and Remigijus Paulavičius

Institute of Data Science and Digital Technologies, Faculty of Mathematics and Informatics, Vilnius University, Akademijos Str. 4, LT-08412 Vilnius, Lithuania; vaiva717@gmail.com (V.P.); mindaugas.juodis@mif.vu.lt (M.J.); remigijus.paulavicius@mif.vu.lt (R.P.)
* Correspondence: ernestas.filatovas@mif.vu.lt

Abstract: Bitcoin's role in global finance has rapidly expanded with increasing institutional participation, prompting new questions about its linkage to macroeconomic variables. This study thoughtfully integrates a Bayesian Markov Chain Monte Carlo (MCMC) covariate selection process within homogeneous and non-homogeneous Hidden Markov Models (HMMs) to analyze 16 macroeconomic and Bitcoin-specific factors from 2016 to 2024. The proposed method integrates likelihood penalties to refine variable selection and employs a rolling-window bootstrap procedure for 1-, 5-, and 30-step-ahead forecasting. Results indicate a fundamental shift: while early Bitcoin pricing was primarily driven by technical and supply-side factors (e.g., halving cycles, trading volume), later periods exhibit stronger ties to macroeconomic indicators such as exchange rates and major stock indices. Heightened volatility aligns with significant events—including regulatory changes and institutional announcements—underscoring Bitcoin's evolving market structure. These findings demonstrate that integrating Bayesian MCMC within a regime-switching model provides robust insights into Bitcoin's deepening connection with traditional financial forces.

Keywords: Bitcoin price dynamics; Bayesian Markov Chain Monte Carlo (MCMC); Hidden Markov Models (HMMs); regime-switching models; macroeconomic determinants; cryptocurrency forecasting

MSC: 60J20; 37N40

1. Introduction

Blockchain technology, originally introduced with Bitcoin [1], has rapidly evolved, finding diverse applications across various sectors such as finance, artificial intelligence, supply chain management, healthcare, and governance [2–5]. Despite significant technological advances and its transformative impact on decentralization across multiple domains [6], cryptocurrency investment and speculation continue to dominate its primary use case, with Bitcoin remaining at the forefront of this movement.

Initially driven primarily by speculative retail investors, Bitcoin's price behavior was characterized by high sentiment sensitivity, low liquidity, and notable market inefficiencies, resulting in substantial volatility and frequent price bubbles [7]. However, over recent years, increasing institutional adoption, regulatory developments, and deeper integration within traditional financial systems have significantly reshaped its market structure. The entry of major financial institutions such as MicroStrategy, Goldman Sachs, and BlackRock, together with regulatory milestones including the Markets in Crypto-Assets Regulation (MiCA) implemented in the European Union and the SEC's approval of Bitcoin spot ETFs in 2024,

has solidified Bitcoin's status as a recognized asset class. Additionally, sovereign adoption—highlighted notably by El Salvador's decision to adopt Bitcoin as legal tender in 2021—underscores its growing significance within the global financial ecosystem. Collectively, these developments represent a shift in Bitcoin's fundamental price dynamics, suggesting that macroeconomic conditions now play an increasingly influential role as the market matures toward efficiency [8].

Despite this evolution, the academic debate regarding the primary drivers of Bitcoin's price remains ongoing and inconclusive. Some studies contend that Bitcoin has increasingly integrated with traditional financial markets, exhibiting stronger correlations with conventional indicators such as stock indices and exchange rates, particularly in the post-COVID-19 environment [9,10]. In contrast, other research emphasizes Bitcoin's continuing autonomy as an asset, arguing that internal ecosystem dynamics, including trading volume, miner activities, and speculative sentiment, remain central to its price formation [9–11]. Additionally, historical event-driven analyses highlight that market manipulation, regulatory developments, and halving events have consistently contributed to Bitcoin's volatility and market dynamics [12,13]. These divergent findings underscore the complexity of Bitcoin's price behavior, suggesting that its determinants are not static but rather dynamic and may vary significantly across different market regimes.

A two-state Hidden Markov Model (HMM) framework is particularly suited for investigating the evolving determinants of Bitcoin's price, as it accommodates latent regime shifts characteristic of financial time series. This framework enables the dynamic assessment of Bitcoin's sensitivity to macroeconomic and internal factors across varying market conditions. Formally, the observed price series Y_t is modeled as conditionally Gaussian, dependent on an unobserved state sequence Z_t following a Markov process:

$$Y_t \mid Z_t = s, \mathbf{X}_t \sim \mathcal{N}\left(\mathbf{X}_t^\top \mathbf{B}_s, \sigma_s^2\right), \quad s = 1, 2, \tag{1}$$

where Z_t denotes the hidden market state (e.g., bullish ($s = 1$) or bearish ($s = 2$)) and $\mathbf{X}_t$ represents macroeconomic, financial, and Bitcoin-specific covariates. The impact of these covariates on Bitcoin's price is governed by a state-dependent coefficient vector $\mathbf{B}_s$, enabling distinct predictors to influence price behavior differently across market regimes.

In a homogeneous HMM, the transitions between states occur with fixed probabilities:

$$P(Z_{t+1} = j \mid Z_t = i) = p_{ij}, \quad i, j = 1, 2, \tag{2}$$

where p_{ij} is the time-invariant probability of transitioning from state i to state j. This structure assumes that market regime shifts follow an internal process independent of external influences.

Conversely, the non-homogeneous HMM (NH-HMM) allows for external variables to dynamically influence state transitions, modeling these probabilities as a function of covariates:

$$P(Z_{t+1} = j \mid Z_t = i, \mathbf{X}_t^{(2)}) = \frac{\exp\left(\mathbf{X}_t^{(2)\top} \boldsymbol{\beta}_{ij}\right)}{\sum_{k=1}^{2} \exp\left(\mathbf{X}_t^{(2)\top} \boldsymbol{\beta}_{ik}\right)}, \quad i, j = 1, 2, \tag{3}$$

where $\mathbf{X}_t^{(2)}$ is a set of covariates influencing the probability of state transitions and $\boldsymbol{\beta}_{ij}$ are logistic regression coefficients.

By capturing these hidden regime shifts, the HMM framework offers a structured approach to analyzing Bitcoin's evolving price dynamics. As institutional involvement increases and market conditions continue to shift, a crucial research question arises: Has

Bitcoin become increasingly intertwined with macroeconomic factors as its market evolves and matures?

To investigate this question, the study employs two complementary approaches: a Bayesian Markov Chain Monte Carlo (MCMC) covariate selection method to identify relevant long-term determinants, and a bootstrapped rolling-window forecasting technique to capture short-term dynamics.

Several studies have already explored Bitcoin price dynamics using Hidden Markov Models (HMMs) and related regime-switching frameworks. Koki et al. [14,15] applied a NH-HMM with Pólya–Gamma augmentation and found that macroeconomic variables were insufficient for reliable out-of-sample prediction, suggesting Bitcoin's relative autonomy from broader economic trends. In contrast, Chen [16] combined vector error correction (VEC) and Markov-switching models, concluding that financial expectations and exchange rates had a stronger influence on Bitcoin price movements than blockchain-specific variables, although the impact varied across "bull" and "bear" market regimes. Katsiampa [17] modeled Bitcoin volatility through Markov-switching GARCH models, revealing distinct regime changes in volatility behavior. Tiwari et al. [18] employed a two-state Markov-switching framework to analyze Bitcoin's speculative bubbles, identifying alternating phases of exuberance and correction. Kodama et al. [19] applied HMMs to detect trend reversals in Bitcoin markets, while Alam and Dutta [20] investigated cryptocurrency interconnectedness across different market regimes. Similarly, Bouri et al. [21] examined regime-dependent spillovers between Bitcoin and traditional financial assets. While these studies highlight the utility of regime-switching models for capturing Bitcoin's nonlinear dynamics, few explicitly incorporate a systematic covariate selection process to assess macroeconomic influences within an HMM framework.

Our study addresses this gap by integrating Bayesian MCMC covariate selection into both homogeneous and non-homogeneous HMMs to trace how Bitcoin's price drivers evolve across hidden market states. Although previous research has examined Bitcoin's price determinants, there is still no consensus on whether these factors remain stable or shift across different market regimes. By embedding Bayesian MCMC within a regime-switching structure, this research offers a new perspective on the dynamic interplay between macroeconomic and Bitcoin-specific variables under varying market conditions. The findings provide valuable insights for investors, regulators, and policymakers, enhancing their understanding of Bitcoin's evolving role within the broader financial system and informing strategic and regulatory decision-making.

The key contributions of this study include:

1. **Identification of Regime-Dependent Determinants:** The analysis reveals how the influence of macroeconomic, financial, and Bitcoin-specific variables changes across market regimes, enriching the understanding of Bitcoin's evolving price behavior.
2. **Enhanced Bayesian MCMC Approach:** The study advances existing Bayesian MCMC covariate selection techniques [14], particularly for regime-switching contexts, to more accurately capture long-term effects.
3. **Improved Predictive Performance:** By employing a bootstrapped rolling-window forecasting approach across different subsamples, the study demonstrates variations in Bitcoin's price predictability under diverse market conditions, thus enhancing forecasting accuracy and reliability.

The paper is structured as follows: Section 2 introduces the Bayesian MCMC covariate selection algorithm, outlines the bootstrapped rolling-window forecasting methodology, and provides an overview of the empirical data used in the study. Section 3 presents and discusses the empirical findings across different subsamples. Section 4 highlights the methodological enhancements and contributions of this research and suggests av-

enues for future research. Section 5 concludes the study by summarizing the key findings and implications.

2. Materials and Methods

This section outlines the methodological approach used to analyze long-term and short-term determinants of Bitcoin's price, illustrated visually in Figure 1.
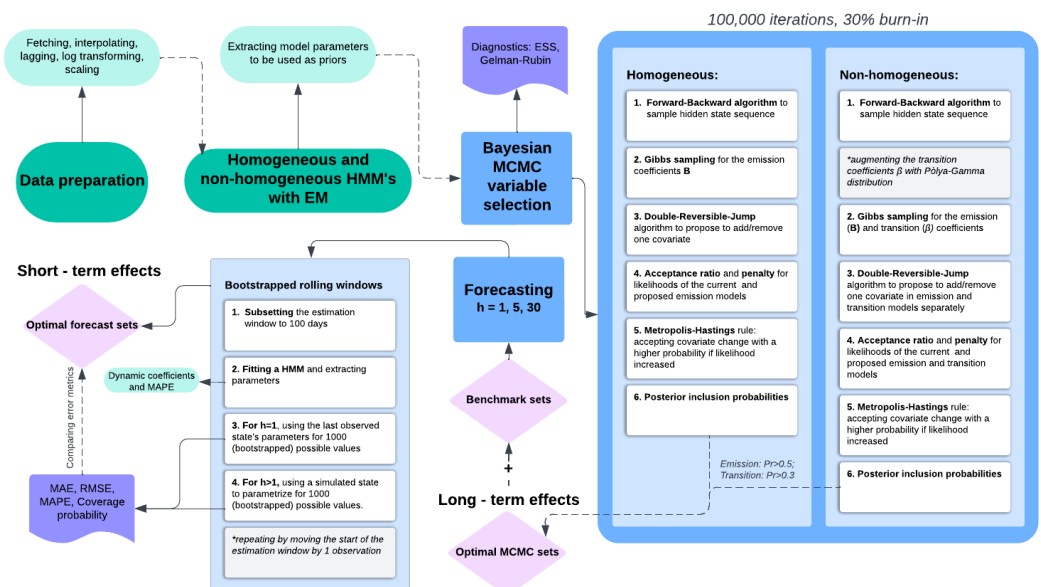
Figure 1. Methodological framework of the analysis, illustrating the integration of Bayesian MCMC covariate selection for identifying key long-term determinants and the bootstrapped rolling-window forecasting procedure for evaluating their predictive performance relative to benchmark covariate sets in capturing Bitcoin's short-term price dynamics.

The analysis comprises three main stages:

1. Data processing and specification of prior parameters;
2. Identification of optimal long-term covariates using the Bayesian MCMC covariate selection algorithm;
3. Evaluation of these selected covariates against benchmark sets through a bootstrapped rolling-window forecasting procedure, considering $h = 1, 5, 30$ steps ahead.

Details of the Bayesian MCMC covariate selection method and its modifications are provided in Section 2.1. The bootstrapped rolling-window forecasting approach is described in Section 2.2. Finally, Section 2.3 presents an overview of the dataset used for empirical analysis.

2.1. The Bayesian MCMC Covariate Selection Algorithm

The optimal subset **X** of covariates for the HMMs is determined using a MCMC algorithm inspired by Koki et al. [14], implemented over 100,000 iterations. This procedure systematically explores the model space to identify the most relevant covariates by repeatedly proposing subsets, simulating hidden states, sampling emission coefficients (and transition coefficients in the non-homogeneous case), calculating and comparing likelihoods, and updating covariate sets accordingly. The procedure begins by fitting a full-covariate HMM using the Expectation–Maximization (EM) algorithm to establish initial parameter priors. The steps are as follows:

1. **Simulating the Latent State Sequence**: The latent states are simulated using the *Forward–Backward* algorithm. Forward probabilities are calculated as

$$\alpha_t(i) = P(Z_t = i \mid \theta, y_{1:t}), \quad i = 1, 2; \quad \theta = (\mathbf{B}, \sigma).$$

   These probabilities inform the computation of backward probabilities from which the hidden state sequence Z_t is subsequently sampled.

2. **Sampling Emission Coefficients**: Emission coefficients $\mathbf{B}_s$ are sampled through a *Gibbs sampling* approach from a *Normal–Inverse Gamma* distribution:

$$\mathbf{B}_s \mid \sigma_s^2, \mathbf{X}, Y \sim \mathcal{N}(\mu_{\mathbf{B}_s}, \Sigma_{\mathbf{B}_s}), \quad \sigma_s^2 \mid \mathbf{B}_s, Y \sim \text{IG}(a, b).$$

   Here, $\mu_{\mathbf{B}_s}$ and $\Sigma_{\mathbf{B}_s}$ represent posterior mean and covariance matrices, while σ_s^2 denotes the state-specific variance drawn from an Inverse–Gamma distribution.

3. **Sampling Transition Coefficients (NH-HMM)**: In the NH-HMM case, transition coefficients $\boldsymbol{\beta}_{ij}$ are sampled using *Pólya–Gamma* augmentation. This method simplifies coefficient sampling by introducing auxiliary Pólya–Gamma distributed latent variables ω_s, enabling efficient Gibbs sampling of transition parameters:

$$\boldsymbol{\beta}_s \mid \omega_s, \mathbf{X}^{(2)}, Z \sim \mathcal{N}(\mu_{\boldsymbol{\beta}_s}, \Sigma_{\boldsymbol{\beta}_s}), \quad \omega_s \sim \mathcal{PG}(b, \mathbf{X}^{(2)}).$$

   Here, $\mu_{\boldsymbol{\beta}_s}$ and $\Sigma_{\boldsymbol{\beta}_s}$ indicate posterior means and covariance matrices.

4. **Double Reversible Jump Algorithm**: The algorithm employs a *Double Reversible Jump* procedure that iteratively proposes adding or removing covariates. Each proposal is evaluated by calculating an acceptance ratio α, which balances model complexity and goodness of fit:

$$\alpha = \frac{p(Y \mid \mathbf{X}_{\text{new}})}{p(Y \mid \mathbf{X}_{\text{old}})} \exp(-pen),$$

   where *pen* is a penalty term proportional to the model's complexity. This penalty discourages overly complex models unless they significantly enhance the model's explanatory power. Through successive iterations, the algorithm efficiently identifies the optimal covariate subset.

5. **Metropolis–Hastings Acceptance Criterion**: The acceptance of the proposed covariate set update follows the *Metropolis–Hastings* criterion, accepting models with $\alpha \geq 1$ automatically, or probabilistically accepting updates with probability α if a random draw $u \sim \mathcal{U}(0, 1)$ is less than α. This approach ensures thorough exploration of model space, promoting convergence to a well-fitting, parsimonious model.

The final set of covariates selected for the emission models is determined based on posterior inclusion probabilities derived from the Bayesian MCMC algorithm. Covariates with high posterior inclusion probabilities (indicating improvement in model fit) are retained, while those with probabilities below a threshold are excluded. Specifically, covariates are selected based on their posterior inclusion probability, with a threshold adapted for emission models (0.5) and a lower threshold for transition models (due to the complexity and subtlety of non-linear effects, set at 0.3).

The choice of 0.5 for the emission models follows standard practice in Bayesian variable selection (e.g., [22]), where inclusion is favored once the posterior probability exceeds the point of equal odds between inclusion and exclusion. In contrast, transition models within NH-HMMs often exhibit weaker and less stable covariate effects due to the inherent challenges of estimating time-varying transition probabilities, as discussed in Section 4. To account for these identifiability issues and prevent the transition models

from becoming overly sparse, thereby excluding potentially relevant predictors, we apply a more permissive threshold of 0.3 for covariate inclusion in the transition equations.

The *Double Reversible Jump* algorithm manages the exploration of a lengthy, correlated candidate covariate list. However, this complexity can cause the algorithm to become stuck in regions of high likelihood early on, making it reluctant to exclude covariates despite their limited contribution. To mitigate this issue, the procedure initializes with a reduced set (contrary to Koki et al. [14]) of three essential covariates, enhancing the algorithm's flexibility in exploring the covariate space. Remaining covariates stay candidates for inclusion or exclusion from the second iteration onward, thus gradually refining the covariate set without overwhelming the algorithm.

Because HMM likelihoods naturally tend to improve when introducing additional covariates—regardless of whether these covariates meaningfully contribute to predictive performance—a penalty-based approach is employed. Specifically, the Double Reversible Jump algorithm introduces a complexity penalty into the acceptance ratio calculation whenever a proposed model includes more covariates than the current model. A penalty of 0.1 was selected to sufficiently discourage overfitting by excessively large covariate sets, balancing model parsimony and exploratory power. This penalty reduces the Metropolis–Hastings criterion acceptance probability for model updates that significantly increase complexity without proportionate improvement in model fit. The choice of this value is motivated by the need to avoid spurious inclusion of redundant predictors, as observed in correlated variable groups, where joint inclusion would otherwise be frequently accepted due to minor cumulative likelihood gains.

To facilitate gradual model refinement and avoid excessively restrictive moves that could trap the chain in local modes, a smaller penalty of 0.05 is imposed for incremental changes (e.g., the addition or removal of a single covariate). This softer penalty for small steps encourages local exploration while maintaining overall control over model complexity. Both penalty values are calibrated empirically, following the observation that higher penalties overly constrained the model space. Compared to previous implementations of [14] without penalization, this refinement substantially reduces the risk of multicollinearity-driven overfitting.

Given that initial iterations may be biased due to insufficient exploration of the parameter space, a burn-in period is implemented, discarding the first 30% of iterations. This percentage ensures the exclusion of early iterations heavily influenced by initial priors, enhancing the stability and reliability of posterior inference. Convergence of the MCMC algorithm is evaluated using diagnostic tools provided by the *coda* 0.19–4.1 package in *R* 4.4.3, including trace plots, the Gelman–Rubin statistic (for comparing variance between chains), and the Effective Sample Size (ESS) to quantify the number of effectively independent samples in the chain. As substantiated later by the typical convergence patterns shown in Section 3.1, the 30% burn-in proportion is sufficient for the majority of the MCMC chains, with 78 out of 96 achieving convergence within this window. Conversely, a longer burn-in period does not resolve convergence issues in the remaining cases, where the Gelman–Rubin statistic remains consistently high across all iterations.

In non-homogeneous Hidden Markov Models (NH-HMMs), sampling transition coefficients β_{ij} poses computational challenges due to the nonlinear nature of logistic regression. To address these challenges, a Pólya–Gamma augmentation approach (Polson et al. [23]) is implemented, introducing latent variables ω_s from a Pólya–Gamma distribution. This transformation simplifies the logistic likelihood into a Gaussian form, significantly improving computational efficiency, mixing properties, and convergence speed within the MCMC sampling process.

2.2. The Forecasting Procedure

As depicted in Figure 1, the *h*-step-ahead forecasting methodology employed in this study integrates a rolling-window approach, initially proposed by Box and Jenkins [24], with bootstrapping techniques introduced by Efron [25]. This combined procedure involves iteratively moving forward a fixed-length window of the most recent observations. Within each window, a HMM is fitted to classify market regimes, estimate model parameters, and determine state transition probabilities. The estimated parameters are then utilized for generating forecasts *h*-steps ahead, specifically the following:

- **For $h = 1$:** Given the most recently observed hidden state, the next-day forecast is obtained as the mean of 1000 bootstrap simulations generated using the respective state-specific parameters.
- **For $h > 1$:** At each forecast horizon beyond one step, the next possible hidden state is simulated using the estimated transition probability matrix. This simulation determines which state-specific parameters to apply for subsequent forecasting.
- **NH-HMM case**: Transition probabilities are dynamic and depend on external covariates. A logistic function employing covariate data determines the transition probability matrix for each forecast step, thus simulating the next possible hidden state.
- At each step, the estimation window is shifted forward by one observation, repeating the forecasting procedure iteratively.

For each bootstrap iteration, the forecast is initiated from the most recent hidden state estimated from the model's posterior distribution. Subsequent state transitions are simulated based on the model's transition probabilities. Forecasted values for each *h*-step-ahead period are derived using the emission parameters $\mathbf{B}_s$ and σ_s, conditioned on the simulated hidden states. This bootstrapping approach generates a distribution of future values, allowing computation of mean forecasts and associated confidence intervals. In the NH-HMM scenario, the recalculation of transition probabilities at each step based on time-varying covariates enhances the model's responsiveness to external influences on market dynamics.

Forecast accuracy and robustness are evaluated using multiple performance metrics, including Mean Absolute Error (MAE), Root Mean Squared Error (RMSE), Mean Absolute Percentage Error (MAPE), and the coverage probability of the 95% forecast confidence intervals relative to the observed actual values.

2.3. Data Considered

The dataset employed in this study consists of daily closing Bitcoin prices spanning from 1 June 2016 to 1 December 2024. To better understand temporal variations in Bitcoin's behavior, the analysis is conducted on two distinct subsamples: the *early* period (1 June 2016 to 31 August 2019) and the *recent* period (1 September 2019 to 1 December 2024).

The Bayesian MCMC analysis incorporates 16 covariates representing financial, macroeconomic, and Bitcoin-specific factors. Data sources include *Yahoo Finance* (accessed via the *tidyquant* package in *R*) and the *Blockchain.com* API. Given sensitivity to varying data magnitudes, all covariates are log-transformed and scaled. Variables unavailable on weekends or those reported with minor lags are aligned to daily frequency using linear interpolation. Additionally, all covariates are lagged by seven days, reflecting a realistic time adjustment period. Table 1 summarizes these adjusted covariates classified into macroeconomic and Bitcoin-specific categories.

Table 1. Summary of variables analyzed, including sources, types, median, minimum, maximum values, and ranges.

Variable	Full Name	Source	Type	Median	Min	Max	Range
BTC_USD	Bitcoin price	Yahoo Finance	-	−0.02	−2.38	1.60	3.98
DJI	Dow Jones Index	Yahoo Finance	Macroeconomic	0.00	−2.28	1.98	4.27
IXIC	Nasdaq index	Yahoo Finance	Macroeconomic	0.19	−2.07	1.81	3.88
SPX	S&P500 index	Yahoo Finance	Macroeconomic	−0.05	−1.91	2.04	3.95
VIX	VIX uncertainty index	Yahoo Finance	Macroeconomic	−0.13	−1.83	4.50	6.33
INFL	Inflation expectations	Calculated	Macroeconomic	0.11	−8.74	2.05	10.80
CNYUSD	CNY/USD exchange rate	Yahoo Finance	Macroeconomic	−0.17	−1.79	2.01	3.80
EURUSD	EUR/USD exchange rate	Yahoo Finance	Macroeconomic	−0.07	−3.15	2.25	5.40
GBPUSD	GBP/USD exchange rate	Yahoo Finance	Macroeconomic	0.01	−3.91	2.91	6.82
JPYUSD	JPY/USD exchange rate	Yahoo Finance	Macroeconomic	0.48	−2.36	1.34	3.70
GC_F	Gold futures	Yahoo Finance	Macroeconomic	0.28	−1.69	2.52	4.21
CL_F	Crude Oil futures	Yahoo Finance	Macroeconomic	0.10	−12.75	2.14	14.90
VOL	Bitcoin trading volume	Yahoo Finance	Bitcoin−specific	0.36	−3.12	1.97	5.09
BLOCK	Average block size	Blockchain.com	Bitcoin−specific	−0.02	−3.84	2.62	6.46
HASH	Total hash rate	Blockchain.com	Bitcoin−specific	0.27	−2.34	1.39	3.73
MINER	Miner revenue	Blockchain.com	Bitcoin−specific	0.17	−2.75	1.94	4.69
HALVING	Days until halving events	Calculated	Bitcoin−specific	0.02	−1.72	1.61	3.33

The selection of macroeconomic covariates is directly motivated by the central research question of this study: Has Bitcoin become increasingly intertwined with macroeconomic factors as its market evolves and matures? Figure 2 visualizes transformed macroeconomic variables alongside Bitcoin's price. Stock market indices (S&P500, Dow Jones, Nasdaq) serve as proxies for investor confidence and broader financial market performance, where positive equity returns may signal economic optimism and greater liquidity, potentially supporting speculative investment across asset classes, including cryptocurrencies. Conversely, the VIX index, a measure of implied stock market volatility, captures risk-off environments where uncertainty may influence portfolio reallocations toward or away from cryptocurrencies. Exchange rates (EUR/USD, GBP/USD, JPY/USD, CNY/USD) reflect international capital flows and monetary policy differentials, offering insight into global liquidity conditions and the strength of reserve currencies relative to Bitcoin. Their inclusion acknowledges Bitcoin's emerging role as both a speculative vehicle and a perceived hedge against fiat currency depreciation in certain regions. Similarly, gold and crude oil futures are included to assess Bitcoin's positioning relative to traditional inflation hedges and commodities, contributing to the broader discussion on whether Bitcoin functions as "digital gold" or aligns more closely with high-risk speculative assets.

The scaled time-series dynamics reveal a pronounced decline in gold prices and inflation expectations following the implementation of COVID-19 regulations in 2020, accompanied by a rise in the VIX uncertainty index, during which Bitcoin's price remained relatively stable. Exchange rates, particularly EUR/USD and GBP/USD, generally exhibit directional alignment with Bitcoin, though they experienced significant declines in 2022 without recovering to their earlier peak levels observed in 2018. Financial market indices, notably the Dow Jones Industrial Index (DJI), exhibit stronger co-movement with Bitcoin's price post 2019, although the magnitude of these movements remains subdued compared to earlier periods.
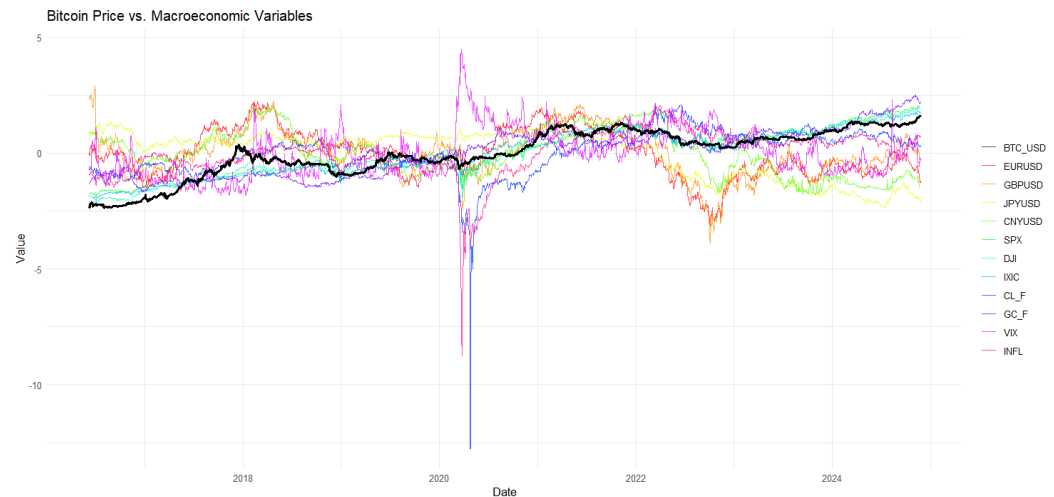
Figure 2. Transformed BTC price (solid black line) and macroeconomic covariates over time.

Figure 3 illustrates Bitcoin-specific variables including trading volume, average block size, total hash rate, miner revenue, and the cyclical variable of days until halving events (set for 9 July 2016, 11 May 2020, 19 April 2024, and 26 March 2028). Bitcoin's price closely tracks trading volume and miner revenue, while days until halving events display a clear cyclical pattern, confirming prior findings by M'bakob [13].
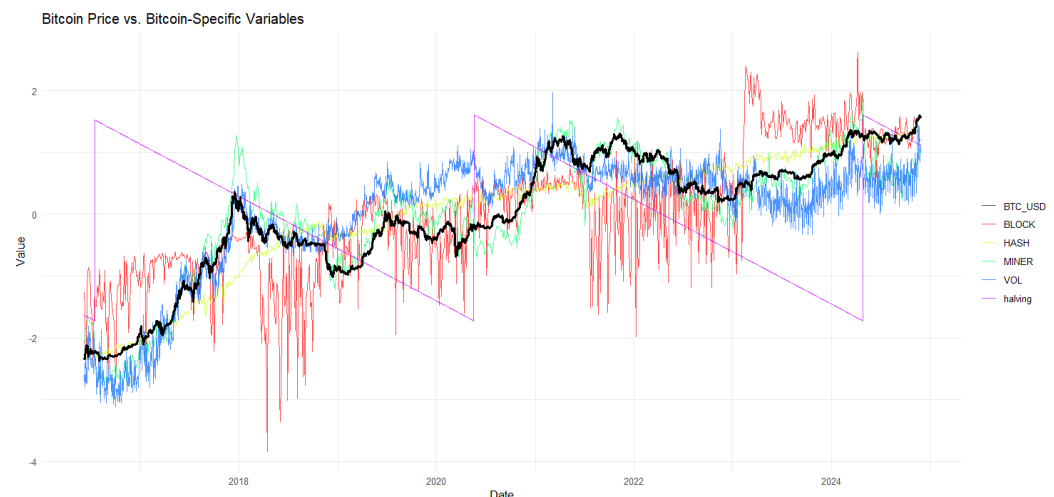

Figure 3. Transformed BTC price (solid black line) and Bitcoin-specific covariates over time.

3. Results

This section presents the empirical findings derived from the Bayesian MCMC covariate selection procedure and the bootstrapped rolling-window forecasting experiments. Key outcomes include identifying the covariates most significantly influencing Bitcoin's price dynamics and evaluating the predictive accuracy for both short-term and long-term forecasts.

3.1. Bayesian MCMC Covariate Selection

Table 2 summarizes the variables selected by the Bayesian MCMC covariate selection algorithm for emission coefficients (**B**) within both homogeneous (HMM) and non-homogeneous (NH-HMM) models, as well as transition coefficients (β) specifically in the NH-HMM. A value of "1" indicates covariates with posterior inclusion probabilities exceeding the threshold of 0.5 for emission coefficients and 0.3 for transition coefficients across different samples and model specifications.

Table 2. Results of Bayesian MCMC covariate selection. A "1" indicates posterior inclusion probabilities surpassing the specified thresholds: ≥ 0.5 for emission coefficients (**B**) and ≥ 0.3 for transition coefficients (β).

Variable	Early			Recent			Full		
	HMM B	NH-HMM B	NH-HMM β	HMM B	NH-HMM B	NH-HMM β	HMM B	NH-HMM B	NH-HMM β
EURUSD	0	0	1	0	1	1	0	0	0
GBPUSD	0	0	0	1	0	0	0	1	0
JPYUSD	0	0	0	0	0	0	0	0	0
CNYUSD	0	0	0	1	1	0	1	0	0
SPX	0	0	0	0	0	0	0	0	0
DJI	0	0	0	0	1	0	0	0	0
IXIC	0	0	0	0	0	0	0	0	0
CL_F	0	0	0	0	0	1	0	0	0
GC_F	1	0	0	0	0	0	0	0	0
VIX	0	0	1	0	0	0	0	0	1
INFL	1	0	0	0	0	0	1	0	0
BLOCK	0	0	0	0	0	0	0	0	0
HASH	0	0	0	1	0	0	0	1	0
MINER	0	0	0	0	0	0	0	0	0
VOL	0	1	0	0	0	0	1	0	0
HALVING	1	0	0	0	0	0	0	0	0

The homogeneous HMM identifies a mixture of macroeconomic and Bitcoin-specific determinants for Bitcoin price across different periods, summarized as follows:

- **Early**: GC_F, INFL, HALVING.
- **Recent**: GBPUSD, CNYUSD, HASH.
- **Full**: CNYUSD, INFL, VOL.

In contrast, the non-homogeneous HMM highlights an evolving pattern, shifting from predominantly Bitcoin-specific factors during the early subsample (evidenced by the exclusive selection of trading volume) toward macroeconomic factors dominating in the recent subsample for both emission and transition models. The selected covariates in the NH-HMM model are the following:

- **Early**: VOL (emission), EURUSD, VIX (transition).
- **Recent**: EURUSD, CNYUSD, DJI (emission), EURUSD, CL_F (transition).
- **Full**: GBPUSD, HASH (emission), VIX (transition).

Diagnostics

Multiple diagnostic metrics are used to evaluate the reliability and convergence of the Bayesian MCMC procedure, following Gelman and Rubin [26]. Foremost among these metrics is the *Gelman–Rubin statistic*, also referred to as the *Potential Scale Reduction Factor* (PSRF). This statistic compares within-chain variance to between-chain variance across multiple chains to determine whether they converge on the same posterior distribution. A PSRF value of 1 indicates perfect convergence, whereas values up to 1.2 are typically deemed acceptable for inference.

The Gelman–Rubin statistics in Table 3 indicate that the homogeneous HMM generally converges more smoothly than the NH-HMM due to the latter's additional complexity from time-varying transitions. Certain covariates, such as CNYUSD in the recent and full samples or GC_F in the recent sample, exhibit notably higher PSRF values, likely stemming from large initial effects estimated by the full-covariate Expectation–Maximization (EM) initialization.

Table 3. Gelman–Rubin statistics for homogeneous (HMM) and non-homogeneous (NH-HMM) models across different periods. A value of 1 indicates perfect convergence, and values ≤ 1.2 are acceptable.

Variable	Early		Recent		Full	
	HMM	**NH-HMM**	**HMM**	**NH-HMM**	**HMM**	**NH-HMM**
EURUSD	1.01	1.17	1.28	1.23	1.44	1.28
GBPUSD	1.14	1.11	1.02	1.11	1.18	1.90
JPYUSD	1.15	1.08	1.04	1.09	1.00	1.13
CNYUSD	1.00	1.11	1.95	2.70	1.80	1.21
SPX	1.00	1.08	1.00	1.09	1.00	1.14
DJI	1.00	1.08	1.00	2.32	1.00	1.14
IXIC	1.00	1.07	1.00	1.12	1.00	1.15
CL_F	1.02	1.12	1.03	1.19	1.15	1.20
GC_F	1.91	1.22	1.00	1.09	1.00	1.14
VIX	1.00	1.18	1.07	1.12	1.01	1.19
INFL	1.04	1.09	1.00	1.13	1.63	1.21
BLOCK	1.00	1.09	1.00	1.10	1.00	1.14
HASH	1.02	1.09	1.01	1.09	1.00	2.17
MINER	1.00	1.11	1.00	1.09	1.00	1.10
VOL	1.00	7.19	1.11	1.15	1.06	1.11
HALVING	1.45	1.07	1.06	1.07	1.00	1.26

Nevertheless, these variables display high posterior inclusion probabilities, suggesting that their high PSRF values reflect meaningful informational content rather than mere noise. In addition, elevated PSRF values are observed for the intercept term, which is less consequential because the intercept remains included by default in subsequent forecasting stages, circumventing the variable selection process.

Figure 4 provides further insight into convergence patterns over time. In the left panels, variables such as HASH (recent HMM) and VOL (full NH-HMM) quickly converge to PSRF = 1 and remain stable. By contrast, the center panels highlight instances in which the PSRF stays high but steady, implying persistent difficulties in achieving full convergence. The right panels, featuring EURUSD data, illustrate a delayed convergence trajectory, wherein the PSRF initially spikes before gradually declining in later iterations.
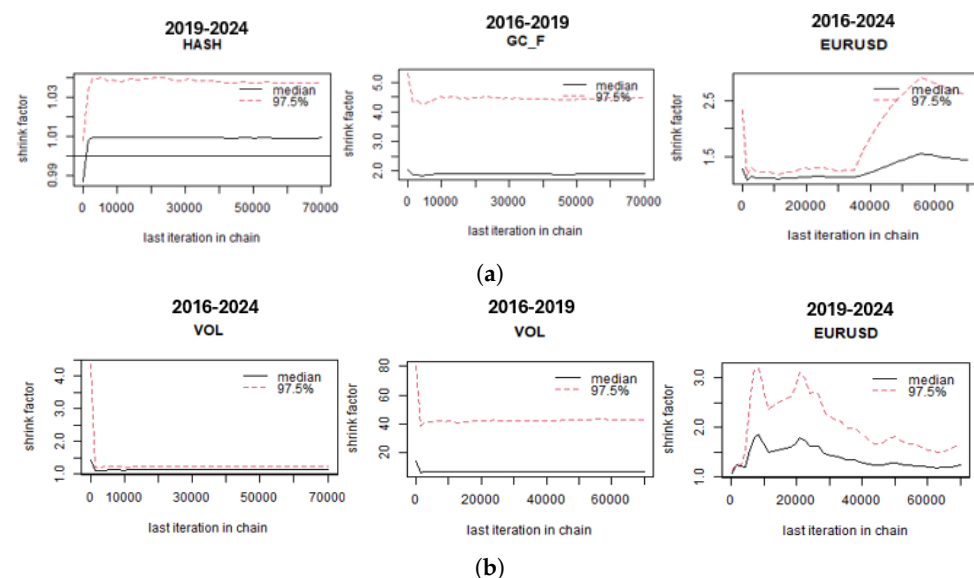

Figure 4. Examples of dynamic Gelman–Rubin statistic plots over the course of MCMC iterations. The solid black line denotes the statistic, whereas the red dashed line represents the 97.5% upper confidence bound. Panel (**a**) depicts typical examples from the HMM procedure; panel (**b**) focuses on NH-HMM cases.

To further assess mixing and autocorrelation, the *Effective Sample Size* (ESS) is computed for each chain. Higher ESS values generally indicate better mixing, ideally approaching the total number of iterations after burn-in (70,000 in this study). The homogeneous HMM tends to maintain ESS values close to this upper bound, apart from certain exceptions, such as EURUSD in the full sample. Conversely, NH-HMM transition models often exhibit lower ESS values, reflecting the inherent challenges of sampling non-linear transition parameters. Detailed ESS outcomes can be found in Appendix A.

3.2. Forecasting

This section presents the rolling-window forecasting approach described in Section 2.2, using the final covariate sets determined by the Bayesian MCMC procedure. Each *h*-step-ahead forecast is based on 1000 bootstrap iterations. A rolling window of 100 observations is selected, motivated by prior evidence that a single hidden state typically persists for 30–60 days, thereby ensuring each window captures both states.

Non-convergence issues occasionally arise during NH-HMM training, triggered by factors such as extreme data values, limited variation among covariates, or pronounced state imbalance. When convergence fails, parameter estimates are unavailable for bootstrapping. In these cases, the affected iteration is skipped, linear interpolation is applied to fill the resulting gap in the forecasted time series, and these interpolated values are retained in subsequent performance metrics. Importantly, these non-convergence instances are rare, with fewer than 10 occurrences across all forecast windows (representing less than 1% of the windows in the shortest subsample). Given their infrequency, this interpolation procedure has a negligible impact on the overall performance metrics. Moreover, linear interpolation provides a conservative estimate that follows the local trend of the original forecast trajectory, minimizing the risk of artificially inflating or distorting error calculations.

Departing from Koki et al. [15], the final MCMC-based covariate sets (Section 3.1) are compared against additional benchmark sets prompted by interim findings and relevant literature:

- **Set 1**: A mixed set of variables (CNYUSD, DJI, GC_F, VOL), following [16,27].
- **Set 2**: Bitcoin-specific variables only (MINER, HASH, VOL, HALVING), as in [28,29].
- **Transmission Covariate for NH-HMM Benchmarks**: VIX is used in both Set 1 and Set 2 for non-homogeneous forecasts, reflecting the importance of uncertainty indices [30,31].

Table 4 presents typical performance ranges for MAE, RMSE, MAPE, and coverage probability (COV. P.) across 1-, 5-, and 30-step horizons in the context of this study. These metrics account for log-transformed Bitcoin prices to mitigate raw error magnitudes and stabilize outliers in MAPE. Previous research [32–34] documents significant volatility-driven forecast errors over longer horizons, while bootstrap approaches (e.g., rolling windows) can improve interval coverage via parameter uncertainty incorporation [35]. Thus, these ranges serve as approximate guidelines rather than rigid thresholds.

Table 4. Typical performance ranges for MAE, RMSE, MAPE, and coverage probability at varying horizons in this study.

Metric	h = 1	h = 5	h = 30
MAE	0.01–0.10	0.05–0.15	0.10–0.30
RMSE	0.01–0.12	0.06–0.18	0.15–0.40
MAPE	10–25%	20–40%	30–50%
COV. P.	90–95%	80–90%	70–85%

Results are discussed by subsample (early, recent, and full) under both homogeneous (HMM) and non-homogeneous (NH-HMM) modeling frameworks. Illustrative figures show actual versus forecasted values, rolling coefficients, and rolling MAPE series for the one-step-ahead models with the lowest MAPE.

3.2.1. Early Sample

In the early sample (2016–2019), Set 2 (Bitcoin-specific variables) achieves the best accuracy for the homogeneous HMM, as shown in Table 5. This outcome aligns with Ibrahim et al. [28], which also indicates that technical or internal Bitcoin metrics suffice during earlier, more speculative stages of Bitcoin's development. However, the MCMC set (GC_F, INFL, HALVING) comes in a close second for one-step-ahead forecasts. Overall, this subsample has relatively low forecast errors but falls below Table 4 coverage guidelines.

Table 5. Homogeneous HMM bootstrapped rolling forecasts for the early sample (2016–2019). The MCMC set consists of GC_F, INFL, HALVING. The minimum MAPE across each set of horizons (1, 5, 30) is highlighted in **bold**.

	MCMC Set			Set 1			Set 2		
Metric	h = 1	h = 5	h = 30	h = 1	h = 5	h = 30	h = 1	h = 5	h = 30
MAE	0.05	0.08	0.16	0.06	0.08	0.17	0.05	0.07	0.16
RMSE	0.05	0.08	0.18	0.06	0.09	0.20	0.05	0.08	0.18
MAPE	14.01	20.18	42.47	15.79	22.63	49.02	**13.52**	**18.65**	**40.82**
COV. P.	78.74	75.67	57.94	81.68	78.17	58.50	81.98	77.68	58.61

Under the non-homogeneous HMM framework (Table 6), the MCMC set (featuring VOL in the emission model and EURUSD, VIX in transition) performs relatively worse. Meanwhile, Set 2 again achieves lower MAPE, though adding VIX for transition does not yield substantial gains compared to simpler homogeneous variants. Incorporating extra Bitcoin-specific variables (MINER, HASH, HALVING) cuts MAPE from 25.30% to 15.23% (1-step-ahead) yet reduces coverage.

Table 6. NH-HMM bootstrapped rolling forecasts for the early sample, where the MCMC set includes VOL (emission) and EURUSD, VIX (transition). The minimum MAPE across each set of horizons (1, 5, 30) is highlighted in **bold**.

	MCMC Set			Set 1			Set 2		
Metric	h = 1	h = 5	h = 30	h = 1	h = 5	h = 30	h = 1	h = 5	h = 30
MAE	0.09	0.16	0.25	0.07	0.13	0.22	0.06	0.12	0.21
RMSE	0.09	0.18	0.27	0.07	0.14	0.25	0.06	0.14	0.24
MAPE	25.30	45.66	70.47	17.69	37.58	61.80	**15.23**	**29.24**	**52.89**
COV. P.	80.74	72.93	54.49	75.05	72.12	56.40	74.61	71.85	53.26

Figure 5 shows the rolling coefficients from the best-performing homogeneous HMM with Set 2, revealing HALVING as the primary driver from mid-2017 through early 2018. This period aligns with heightened speculation and anticipation of halving's influence on supply [13]. Over time, HALVING's impact diminishes in favor of factors linked to institutional involvement and broader macroeconomic developments.
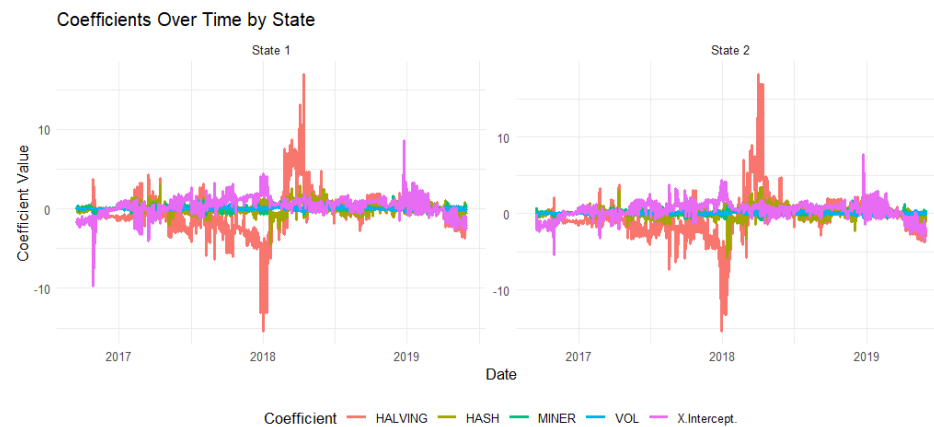
Figure 5. Rolling coefficients in States 1 and 2 for the homogeneous HMM with Set 2, early sample (2016–2019). HALVING dominates during speculative phases, then tapers off.

Figure 6 illustrates sharp MAPE spikes during the 2017–2018 bull run and subsequent crash, underscoring the influence of HALVING, VOL, and HASH in high-volatility regimes. More moderate errors reappear as the market stabilizes. An additional MAPE surge in early 2019 corresponds to the intercept absorbing unexplained volatility. These anomalies match Tether- and PlusToken-related irregularities, consistent with [12].
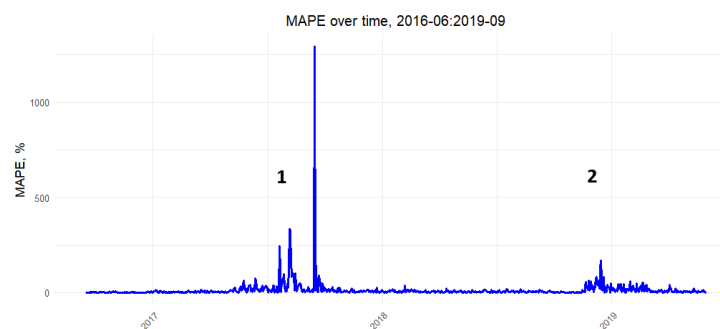

Figure 6. Rolling MAPE for the homogeneous HMM with Set 2 in the early sample. (**1**) Tether issuance and trading (2017–2018); (**2**) PlusToken Ponzi scheme (2019).

3.2.2. Recent Sample

In the recent subsample (2019–2024), Set 1 (macroeconomic + Bitcoin variables) emerges as the best performer for the homogeneous HMM, while the MCMC set (CNYUSD, GBPUSD, HASH) runs a close second at one-step-ahead (Table 7). By contrast, Set 2—dominant in the early sample—now struggles to capture the evolving interplay of traditional financial factors, in line with [27,36]'s findings on Bitcoin's growing macroeconomic sensitivity.

Table 7. Homogeneous HMM forecasts for the recent sample (2019–2024). The MCMC set comprises CNYUSD, GBPUSD, and HASH. The minimum MAPE across each set of horizons (1, 5, 30) is highlighted in **bold**.

	MCMC Set			Set 1			Set 2		
Metric	h = 1	h = 5	h = 30	h = 1	h = 5	h = 30	h = 1	h = 5	h = 30
MAE	0.07	0.09	0.18	0.06	0.09	0.18	0.06	0.09	0.20
RMSE	0.07	0.10	0.21	0.06	0.09	0.21	0.06	0.10	0.23
MAPE	27.61	42.41	102.42	**25.85**	**38.84**	**87.35**	33.69	46.07	107.24
COV. P.	81.77	78.25	60.97	82.56	79.45	60.71	79.20	77.10	60.76

Non-homogeneous forecasts (Table 8) underscore this trend: the MCMC set (DJI, CNYUSD, EURUSD in emission; EURUSD, CL_F in transition) outperforms benchmark sets over shorter horizons but shows weak coverage at longer horizons. Both homogeneous and non-homogeneous results highlight Bitcoin's macroeconomic entanglement post 2019.

Table 8. NH-HMM forecasts for the recent sample, with the MCMC set involving DJI, CNYUSD, EURUSD (emission), and EURUSD, CL_F (transition). The minimum MAPE across each set of horizons (1, 5, 30) is highlighted in **bold**.

Metric	MCMC Set			Set 1			Set 2		
	h = 1	h = 5	h = 30	h = 1	h = 5	h = 30	h = 1	h = 5	h = 30
MAE	0.08	0.15	0.26	0.07	0.14	0.24	0.08	0.25	0.53
RMSE	0.08	0.16	0.29	0.07	0.16	0.27	0.08	0.29	0.62
MAPE	**29.13**	**56.88**	122.43	30.13	58.98	**106.25**	33.80	88.61	172.30
COV. P.	77.81	69.31	44.85	76.07	70.89	51.33	74.58	70.03	53.19

Figure 7 illustrates rolling coefficients for the homogeneous HMM with Set 1. CNYUSD and DJI peak during the 2020–2022 bull run and 2022 volatility surges, while GC_F rises in importance from 2022 onward. VOL remains comparatively stable, suggesting it tracks broader market swings without driving them [27].
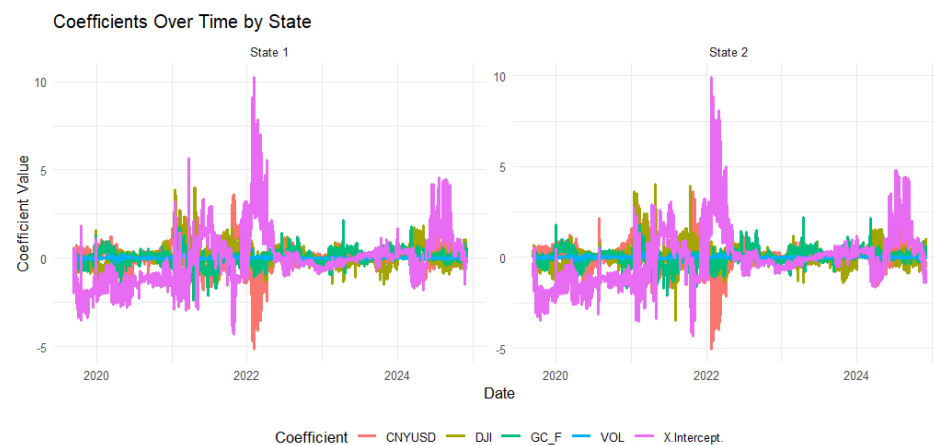

Figure 7. Rolling coefficients in States 1 and 2 for the homogeneous HMM with Set 1, recent sample (2019–2024).

Figure 8 shows generally lower volatility spikes than in the early sample, though large MAPE jumps occur in 2022 and 2023, coinciding with events such as BlackRock's Bitcoin ETF filing and the EU's *Markets in Crypto-Assets Regulation* (MiCA) legislation. Investor sentiment, beyond the scope of these models, likely contributes to abrupt shifts in price.
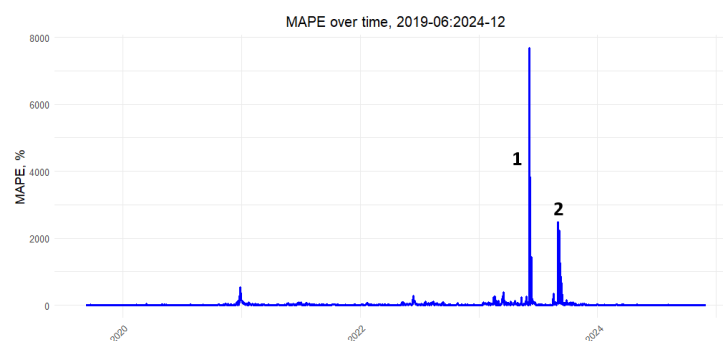

Figure 8. Rolling MAPE for the homogeneous HMM with Set 1 in the recent sample. (**1**) BlackRock's spot BTC ETF filing; (**2**) EU's MiCA adoption.

3.2.3. Full Sample

When evaluated over the entire 2016–2024 period, the shorter early sample exerts a pronounced influence. Table 9 indicates that Set 2 (Bitcoin-only) attains the lowest MAPE (15.78%) for the homogeneous HMM, whereas the MCMC set (CNYUSD, INFL, VOL) yields slightly better coverage. Performance converges across sets for 30-step-ahead forecasts, all scoring relatively poorly.

Table 9. Homogeneous HMM forecasts for the full sample (2016–2024). The MCMC set includes CNYUSD, INFL, and VOL. The minimum MAPE across each set of horizons (1, 5, 30) is highlighted in **bold**.

	MCMC Set			Set 1			Set 2		
Metric	**h = 1**	**h = 5**	**h = 30**	**h = 1**	**h = 5**	**h = 30**	**h = 1**	**h = 5**	**h = 30**
MAE	0.04	0.06	0.11	0.04	0.05	0.11	0.03	0.05	0.11
RMSE	0.04	0.06	0.13	0.04	0.06	0.13	0.03	0.06	0.13
MAPE	24.68	31.85	74.70	24.95	28.70	**72.56**	**15.78**	**26.68**	73.14
COV. P.	82.39	78.86	62.65	82.59	78.89	60.20	80.73	77.31	59.69

Under the NH-HMM (Table 10), Set 2 again excels at one-step-ahead horizons with the lowest MAPE (21.26%), but it deteriorates more than other sets at longer forecasts. Set 1 improves for five-step predictions, while the MCMC set (GBPUSD, HASH for emission; VIX for transition) slightly enhances coverage.

Table 10. NH-HMM forecasts for the full sample. The MCMC set includes GBPUSD, HASH (emission) and VIX (transition). The minimum MAPE across each set of horizons (1, 5, 30) is highlighted in **bold**.

	MCMC Set			Set 1			Set 2		
Metric	**h = 1**	**h = 5**	**h = 30**	**h = 1**	**h = 5**	**h = 30**	**h = 1**	**h = 5**	**h = 30**
MAE	0.05	0.10	0.16	0.04	0.09	0.15	0.05	0.12	0.25
RMSE	0.05	0.11	0.18	0.04	0.10	0.17	0.05	0.14	0.29
MAPE	24.08	49.75	**95.82**	21.67	**39.35**	96.30	**21.26**	70.42	116.08
COV. P.	78.16	70.61	51.56	76.61	71.39	51.22	75.01	70.34	53.88

Figure 9 shows the rolling coefficients for the homogeneous HMM with Set 2 across the entire period. Notable spikes in HALVING reflect its cyclical significance around scheduled supply reductions [13]. Volatility in the intercept captures unexplained short-term shocks, while VOL, HASH, and MINER remain comparatively stable, consistent with King [9]'s emphasis on mining variables primarily at threshold events.
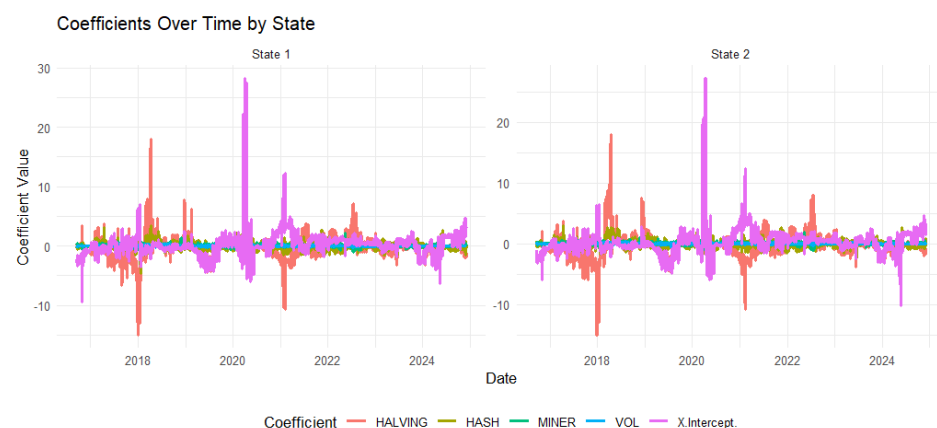

Figure 9. Rolling coefficients for the homogeneous HMM with Set 2 over the full sample (2016–2024).

Figure 10 illustrates why Set 1 loses its advantage at the full-sample level despite strong results in the recent period. High MAPE episodes appear before 2021, suggesting omitted factors or short-term speculative behavior as identified in previous studies [10,19,29]. Nonetheless, the elevated error regions are relatively brief under Set 2, making it favorable overall. Periods labeled (1) and (2) again correspond to Tether issuance/trading and the PlusToken scheme; event (3) denotes the halving impact observed around 2020, when major firms (e.g., MicroStrategy, Square, PayPal) accelerated Bitcoin accumulation.
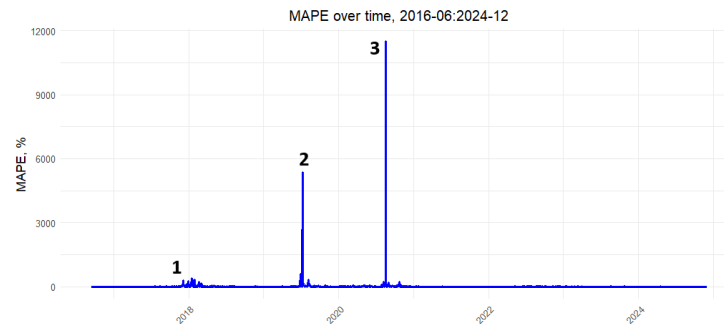

Figure 10. Rolling MAPE for the homogeneous HMM with Set 2 over the full sample. (**1**) Tether trading (2017–2018), (**2**) PlusToken (2019), (**3**) Halving-related demand (2020).

While the proposed framework demonstrates strong performance for short-term forecasts (h = 1, 5), the 30-step-ahead predictions often yield considerably higher MAPE values, exceeding 100% in several subsamples. This reflects the intrinsic challenge of modeling Bitcoin prices over longer horizons due to their high volatility, sensitivity to external shocks, and limited predictability. Accordingly, these long-term forecasts should be viewed as indicative scenario tools rather than precise point predictions. They may still provide useful insights into potential regime shifts or directional tendencies but should be interpreted with caution, especially in practical financial or policy decision-making contexts.

4. Discussion and Methodological Comparisons

The empirical findings from the Bayesian MCMC covariate selection in homogeneous HMMs indicate that both macroeconomic and Bitcoin-specific factors influence Bitcoin's price over the examined periods, underscoring the asset's evolving market structure. By contrast, results from the non-homogeneous HMM highlight a shift from primarily Bitcoin-specific determinants toward macroeconomic drivers, particularly in the later subsample. These observations are further supported by the forecasting procedure, aligning with [16,27,36], where the highest accuracy for the early sample derives from a Bitcoin-focused Set 2, while a mixed Set 1 dominates for the later sample—yet Set 2 still outperforms in the full sample.

Dynamic Coefficients and Market Evolution

Rolling coefficient estimates provide deeper insight into shifting price drivers. In both the early and full-sample analyses, *Days until halving* exhibits a pronounced effect, consistent with [13], which links halving events to significant supply reductions and subsequent price surges. Conversely, in the recent subsample, the *CNY/USD* exchange rate and the *Dow Jones* index assume top coefficient ranges, highlighting Bitcoin's heightened sensitivity to global financial markets, consistent with [31,37].

Additionally, dynamic MAPE values reveal that large forecasting errors coincide with influential external shocks or fraudulent activities [27]. For instance, substantial error spikes appear in June 2023 alongside BlackRock's ETF filing and in April 2023, coinciding

with the EU's MiCA adoption. Likewise, Tether issuance (2017–2018) and the *PlusToken* Ponzi scheme (2019) align with error peaks observed in earlier years [12].

Methodological Extensions and Refinements

Building on [14], this study introduces several modifications designed to enhance covariate selection and forecasting performance:

- *Penalized Acceptance Ratios*: A penalty term is added to discourage unnecessary model complexity.
- *Reduced Initial Covariate List*: Initialization with a minimal set of covariates enhances search flexibility.
- *Lower Posterior Transition Benchmark*: A reduced threshold is used to accommodate non-linear transition effects.
- *Bootstrapped Rolling-Window Forecasting*: Short-term predictions benefit from iterative re-estimation on local windows.

Further innovations include extending the approach to homogeneous HMMs, enlarging the macroeconomic and Bitcoin-specific variable pool, explicitly reporting MCMC diagnostics, and incorporating dynamic, rolling-window analyses. These collective refinements mitigate multicollinearity and overfitting by discouraging redundant covariates. For instance, SPX, DJI, and IXIC—highly correlated U.S. indices—are rarely all included simultaneously, as their combined likelihood improvement triggers the penalty mechanism.

Challenges in Estimating Transition Models

Despite these advancements, sampling transition probabilities within non-homogeneous HMMs remains challenging. Some variables display low ESS and elevated Gelman–Rubin statistics (Diagnostics Section). Among the 96 estimated MCMC chains, 4 exceeded the PSRF convergence threshold of 1.2 in the early subsample, 5 in the recent subsample, and 9 in the full sample, with poor convergence more frequently observed in the NH-HMM specifications. Restrictive priors, or attempts to inflate priors for broader exploration, can yield overflow errors in the logistic transition likelihood if $\mathbf{X}_t^\top \boldsymbol{\beta}_{ij}$ becomes excessively large. Similar complexities are noted in [38], wherein non-linear transitions undermine stable mixing. Although Pólya–Gamma augmentation [23] addresses non-conjugacy issues, time-varying transitions and modest covariate effects can complicate convergence. Empirically, adding the VIX uncertainty index to transition equations often does not enhance accuracy, deviating from [30,31] but aligning with [10], which report limited forecasting gains from uncertainty proxies.

Covariate Selection Versus Forecasting Horizon

Another key observation is that MCMC-selected covariates—optimized for broad, long-term effects—do not consistently surpass benchmark sets under rolling-window forecasts aimed at short-term patterns. In high-correlation scenarios, substituting one macroeconomic or Bitcoin variable for another often yields minimal net likelihood gain. For instance, the non-homogeneous MCMC set (CNYUSD, DJI, EURUSD, CL_F) is closely matched by a slightly different Set 1 (CNYUSD, DJI, GC_F, VOL), emphasizing that strong pairwise correlations can make certain variables interchangeable.

SWOT Analysis of the Methodological Approach

Strengths. The methodological framework—Bayesian MCMC-based variable selection combined with homogeneous and non-homogeneous HMMs—offers several notable strengths. It effectively captures regime-dependent relationships and accommodates structural shifts in Bitcoin's price dynamics. By integrating long- and short-term forecasting through a rolling-window bootstrap procedure, the approach remains flexible to evolving market conditions. The Bayesian framework in particular enhances model parsimony by

using posterior inclusion probabilities, thereby reducing the risk of overfitting in high-dimensional settings.

Weaknesses. Several limitations should be acknowledged. The non-linear nature of transition probabilities in the non-homogeneous HMMs introduces considerable computational challenges, often leading to slower MCMC convergence and lower effective sample sizes. Additionally, the reliance on lagged covariates may limit the model's real-time predictive responsiveness, and the methodological complexity could reduce transparency and interpretability for broader, non-technical audiences.

Opportunities. This framework opens up promising opportunities for extension. It can be adapted to other volatile assets or markets undergoing structural transformation. Future research could explore its integration with sentiment indicators, regime duration modeling, or hybrid machine learning-HMM systems. Moreover, real-time macro-financial surveillance tools based on this framework could aid policymakers and institutional investors.

Threats. Potential threats include the risk of misinterpretation or over-reliance on model outputs, particularly in policymaking or financial regulation. Model performance may degrade rapidly during unprecedented crises (e.g., pandemics or geopolitical shocks) if relevant covariates are omitted or lagged responses are misaligned. Moreover, high computational demands and limited accessibility for practitioners may hinder broader adoption.

Macroeconomic and Regulatory Outlook: A PESTLE Perspective

Beyond statistical and econometric modeling, Bitcoin's long-term evolution is embedded in broader macro-environmental dynamics. A PESTLE framework helps illustrate this multifaceted landscape. *Politically*, Bitcoin faces shifting regulatory positions—ranging from El Salvador's adoption to the European MiCA regulation—affecting global legitimacy. *Economically*, its ties to inflation expectations, institutional investment flows, and interest rate regimes grow stronger. *Socially*, cultural attitudes, generational shifts, and public narratives drive adoption cycles. *Technologically*, innovations like Layer 2 scaling and proof-of-stake alternatives shape user behavior and infrastructure. *Legally*, classification as a commodity or security continues to shape compliance obligations and institutional involvement. *Environmentally*, Bitcoin mining remains under scrutiny due to energy intensity, sparking interest in sustainable practices. These contextual forces deepen Bitcoin's integration into traditional financial systems while also introducing volatility through exogenous shocks.

Policy Implications

The findings of this study suggest that Bitcoin is increasingly influenced by traditional macroeconomic factors, particularly during recent periods of institutional adoption and regulatory attention. Policymakers and financial regulators should consider integrating Bitcoin and other major cryptocurrencies into broader macro-financial surveillance frameworks. The heightened sensitivity of Bitcoin prices to interest rates, exchange rates, and stock market volatility implies that central bank policies and fiscal developments may have amplified spillover effects into the crypto asset space. Therefore, establishing clear, adaptive regulatory frameworks—such as MiCA in the EU or guidelines on exchange-traded products—can help stabilize investor expectations and reduce market uncertainty. Additionally, given the limitations of long-horizon predictability, policy communication strategies should emphasize the inherent risks of speculative behavior, particularly for retail investors.

4.1. Alternative Approaches for Covariate Selection

Given the impact of variable selection on forecast performance, various machine learning methods were tested to gauge their suitability.

4.1.1. Least Absolute Shrinkage and Selection Operator (LASSO)

First, LASSO was applied to the complete covariate set to isolate coefficients shrunk to zero. However, the optimal λ (selected via cross-validation) retained essentially all covariates, reflecting high dimensionality and multicollinearity. Adopting a larger λ (one standard error from the minimum) only excluded *INFL*, which still left too many covariates for the HMM structure, risking overfitting.

4.1.2. Elastic Net

An Elastic Net model with $\alpha = 0.5$ (balancing L1 and L2 penalties) was then employed under cross-validation. Nevertheless, no coefficients were shrunk to zero, paralleling the outcome of LASSO. Thus, while these methods offer efficient shrinkage in conventional regression contexts, they proved unsuitable for HMM-based analyses due to entrenched multicollinearity and regime-switching dynamics.

4.1.3. Random Forest (RF)

A Random Forest algorithm was next used to rank covariates based on reductions in out-of-bag accuracy. The top four—SPX, IXIC, INFL, and DJI—strongly overlapped, capturing similar U.S. financial market trends. Incorporating all four into a rolling HMM forecast induced convergence problems stemming from high correlation among indices. These results reaffirm that solely algorithmic feature ranking must be reconciled with the requirements of HMM-based methods.

4.1.4. Support Vector Machine (SVM)

Finally, a rolling-window SVM was tested on identical covariate sets. Despite the same bootstrap logic, SVM forecasts for 1-day-ahead lagged substantially behind HMM equivalents. For example, a rolling SVM using Set 2 over the full sample produced a MAPE of 29.52%, compared to 15.78% with the homogeneous HMM. Coupled with higher computational expenses, SVM was deemed impractical for the studied regime-switching context.

Implications and Future Directions

Collectively, these alternative strategies highlight the distinctive requirements of HMM-based forecasting. Methods like LASSO or Elastic Net could not adequately reduce the correlated feature space. Random Forest offered feature importance insights but did not address multicollinearity in transition models. Rolling SVM attempts incurred reduced accuracy and heavier computation. In contrast, the Bayesian MCMC approach—tailored for regime-switching—showed robust short-term performance when combined with rolling windows and bootstrapping while also identifying high-impact covariates for the long run.

From a practical standpoint, investors may wish to monitor macroeconomic indicators (e.g., exchange rates, stock indices) alongside Bitcoin-specific metrics (e.g., trading volume, halving cycles) to anticipate major price swings. Policymakers could leverage such insights to understand how cryptocurrencies interface with traditional financial systems, potentially shaping more informed regulatory measures. Future research might extend this work by incorporating structural break detection or investor sentiment variables directly into state transitions, offering a finer-grained view of how exogenous events reshape Bitcoin's market regimes.

5. Conclusions

This paper investigates whether Bitcoin has become increasingly sensitive to macroeconomic variables, especially amid rising institutional adoption. While some studies characterize Bitcoin as an autonomous asset, others posit growing convergence with traditional financial markets. To clarify this debate, the Bayesian MCMC covariate selection method

of [14] was extended to both homogeneous and non-homogeneous Hidden Markov Models (HMMs). This study thoughtfully integrates established techniques—Bayesian MCMC-based covariate selection, regime-switching modeling, and rolling-window forecasting—to address challenges like overfitting, convergence, and predictive instability. While each method individually is well established in the literature, their combined application to the evolving cryptocurrency market offers new empirical insights.

A dataset comprising 16 macroeconomic and Bitcoin-specific variables from 2016 to 2024 was used to compare the MCMC-selected covariate sets against two benchmark sets:

- **Set 1**, a combination of macroeconomic and Bitcoin-specific variables;
- **Set 2**, Bitcoin-focused covariates only.

In non-homogeneous HMMs, the VIX uncertainty index served as a transition covariate. Analyses across an early (pre-2019) and recent (post-2019) period demonstrate a clear evolution in Bitcoin's price determinants. Whereas early Bitcoin price movements were dominated by internal metrics, including trading volume and halving cycles, the recent era shows a stronger influence from macroeconomic indicators, particularly exchange rates and U.S. market indices. Dynamic forecasting errors further reveal that sharp volatility often aligns with regulatory shifts, major institutional announcements, and potential market manipulation or sentiment-driven episodes.

By coupling Bayesian MCMC-based variable selection with rolling-window forecasts, this study contributes a robust framework for uncovering the shifting drivers behind Bitcoin's price dynamics. Practical considerations—such as effectively sampling non-linear transitions or managing high-dimensional covariate sets—proved crucial to the methodology's success.

Future Research

Potential extensions include (i) incorporating Bayesian change-point detection for extreme volatility episodes, (ii) adding sentiment or social-media-based indicators to capture behavioral effects, and (iii) testing structural break hypotheses tied to pivotal regulatory or macroeconomic disruptions. These directions can further refine understanding of how digital assets integrate into—and diverge from—traditional financial systems.

Author Contributions: Conceptualization, V.P., E.F. and R.P.; methodology, V.P.; software, V.P.; validation, V.P., E.F., M.J. and R.P.; formal analysis, V.P., E.F. and R.P.; investigation, V.P.; data curation, V.P.; writing—original draft preparation, V.P.; writing—review and editing, E.F., M.J. and R.P.; visualization, V.P.; supervision, E.F. and R.P. All authors have read and agreed to the published version of the manuscript.

Data Availability Statement: The raw data supporting the conclusions of this article are available in GitHub: https://github.com/vaaiva/BTC_data_prep (accessed on 9 May 2025).

Conflicts of Interest: The authors declare no conflicts of interest.

Appendix A. Extended ESS Analysis

Tables A1–A3 present the Effective Sample Size (ESS) values for the homogeneous HMM (States 1 and 2) and the non-homogeneous HMM (NH-HMM) emission and transition models, respectively. Values approaching 70,000 suggest minimal autocorrelation and strong chain mixing.

For the homogeneous HMM, ESS values generally remain close to the post-burn-in iteration count of 70,000, implying that the chains exhibit limited autocorrelation and reliably sample from the posterior. State 1 and State 2 typically show similar ESS values,

indicating that both states are equally well represented in the chain. An exception is observed for EURUSD in the full sample, where the ESS in State 2 drops as low as 141. Nonetheless, its final posterior inclusion probability remains below the threshold for inclusion in the optimal covariate set.

Regarding the **NH-HMM emission coefficients**, most variables—apart from EURUSD—achieve ESS values close to 70,000. This finding suggests that, despite the added complexity of modeling dynamic transitions, the emission model still manages to sample effectively for most variables. Conversely, the transition model exhibits markedly lower ESS counts, reflecting stronger autocorrelation and the computational challenges associated with non-linear, time-varying transitions. Furthermore, an asymmetry is observed between states: on average, State 2 achieves a lower ESS, indicating that its posterior surface may be more difficult to traverse.

Such behavior is explained in part by differences in the prior specification. For instance, the initial model for State 1 used narrower priors, potentially anchoring the sampler more efficiently around its true posterior mode. By contrast, wider priors in State 2 left the sampler with more parameter space to explore, thereby reducing its ESS. Although these factors complicate the convergence process, they also highlight the capacity of the NH-HMM to capture nuanced, regime-specific phenomena that might be overlooked by a simpler homogeneous approach.

Table A1. ESS values of the MCMC chains in the homogeneous HMM framework across the early, recent, and full subsamples for States 1 and 2. Values near the maximum iteration count (70,000) indicate sufficient chain mixing.

Variable	Early Sample		Recent Sample		Full Sample	
	State 1	State 2	State 1	State 2	State 1	State 2
Intercept	70,000	70,000	70,000	69,220	68,425	70,000
EURUSD	69,498	69,418	70,000	70,000	21,491	141
GBPUSD	70,000	70,000	67,816	70,000	69,314	69,743
JPYUSD	71,748	71,759	70,000	70,000	70,000	70,000
CNYUSD	72,276	72,404	70,000	70,000	70,000	70,000
SPX	70,000	70,000	68,834	68,852	69,665	69,671
DJI	69,135	69,145	70,000	70,000	67,836	67,853
IXIC	70,000	70,000	69,294	69,283	70,000	70,000
CL_F	69,012	69,031	70,000	70,000	70,000	70,000
GC_F	69,242	70,000	67,624	67,628	70,000	70,000
VIX	50,829	53,844	71,405	71,545	70,000	70,000
INFL	70,000	70,000	70,000	70,000	64,784	64,803
BLOCK	70,000	70,000	70,000	70,000	70,000	70,000
HASH	70,000	70,000	70,000	70,000	70,000	70,000
MINER	70,757	70,000	69,895	69,919	70,000	70,000
VOL	70,000	70,000	70,000	70,000	67,510	67,519
HALVING	70,000	70,000	69,380	69,978	70,000	70,000

Table A2. ESS values of the MCMC chains in the non-homogeneous HMM (NH-HMM) framework for the **emission** model, across the early, recent, and full subsamples for States 1 and 2. Values near 70,000 suggest robust mixing.

Variable	Early Sample		Recent Sample		Full Sample	
	State 1	State 2	State 1	State 2	State 1	State 2
Intercept	71,180	70,000	70,777	70,000	71,125	71,232
EURUSD	70,000	70,000	220	74	18,031	18,516
GBPUSD	69,859	70,076	70,000	70,000	70,000	70,000
JPYUSD	70,000	70,000	67,794	67,737	70,820	70,826
CNYUSD	72,008	71,971	52,599	30,452	70,000	70,000
SPX	70,764	70,000	69,200	69,197	70,000	70,000
DJI	70,000	70,000	30,540	30,432	70,000	70,000
IXIC	70,000	70,000	70,000	70,000	68,048	68,028
CL_F	70,000	70,000	71,547	71,563	70,000	70,000
GC_F	70,000	70,000	70,000	70,000	70,000	70,000
VIX	72,342	72,399	70,000	70,000	70,000	70,000
INFL	71,791	71,776	69,012	68,979	71,196	71,183
BLOCK	70,000	70,000	65,919	66,812	70,000	70,000
HASH	71,038	71,075	70,000	70,000	68,700	68,629
MINER	70,000	70,000	70,000	70,000	70,328	70,320
VOL	70,019	70,000	70,000	70,000	70,000	70,000
HALVING	70,000	70,000	70,770	70,840	70,000	70,000

Table A3. ESS values of the MCMC chains in the non-homogeneous HMM (NH-HMM) framework for the **transition** model, across the early, recent, and full subsamples for States 1 and 2. Values near 70,000 suggest robust chain mixing.

Variable	Early Sample		Recent Sample		Full Sample	
	State 1 β	State 2 β	State 1 β	State 2 β	State 1 β	State 2 β
Intercept	68,974	56,564	70,000	23,968	70,000	2226
EURUSD	62,539	5477	71,652	68,769	70,169	68,052
GBPUSD	70,000	70,000	16,679	1905	8971	1926
JPYUSD	70,000	70,000	70,000	70,000	12,816	1938
CNYUSD	70,000	69,246	64,957	54,275	38,085	4513
SPX	70,000	70,000	70,000	70,000	19,021	1686
DJI	70,000	67,015	70,000	68,867	9382	2244
IXIC	70,000	70,000	70,000	70,000	12,397	1801
CL_F	70,000	70,000	46,737	4399	70,000	70,000
GC_F	31,839	7789	70,000	68,838	38,853	3535
VIX	70,000	37,592	70,000	70,000	48,271	6305
INFL	70,000	70,000	20,567	2353	70,000	63,688
BLOCK	70,000	68,980	70,000	70,000	13,147	3602
HASH	69,168	70,000	70,000	65,189	6128	795
MINER	70,000	70,211	70,000	70,000	70,000	70,000
VOL	70,000	70,000	52,374	4409	65,981	63,015
HALVING	68,414	70,000	15,171	2082	67,071	70,000

References

1. Nakamoto, S. Bitcoin: A Peer-to-Peer Electronic Cash System. 2008. Available online: https://bitcoin.org/bitcoin.pdf (accessed on 9 May 2025).
2. Paulavičius, R.; Grigaitis, S.; Igumenov, A.; Filatovas, E. A decade of blockchain: Review of the current status, challenges, and future directions. *Informatica* **2019**, *30*, 729–748. [CrossRef]
3. Filatovas, E.; Marcozzi, M.; Mostarda, L.; Paulavičius, R. A MCDM-based framework for blockchain consensus protocol selection. *Expert Syst. Appl.* **2022**, *204*, 117609. [CrossRef]

4. Orts, F.; Paulavičius, R.; Filatovas, E. Improving the implementation of quantum blockchain based on hypergraphs. *Quantum Inf. Process.* **2023**, *22*, 330. [CrossRef]

5. Marcozzi, M.; Filatovas, E.; Stripinis, L.; Paulavičius, R. Data-Driven Consensus Protocol Classification Using Machine Learning. *Mathematics* **2024**, *12*, 221. [CrossRef]

6. Juodis M.; Filatovas E.; Paulavičius R. Overview and empirical analysis of wealth decentralization in blockchain networks. *ICT Express* **2024**, *10*, 380–386. [CrossRef]

7. Cheah, E.T.; Fry, J. Speculative bubbles in Bitcoin markets? An empirical investigation into the fundamental value of Bitcoin. *Econ. Lett.* **2015**, *130*, 32–36. [CrossRef]

8. Urquhart, A. The inefficiency of Bitcoin. *Econ. Lett.* **2016**, *148*, 80–82. [CrossRef]

9. King, J.C.; Dale, R.; Amigó, J.M. Blockchain metrics and indicators in cryptocurrency trading. *Chaos Solitons Fractals* **2024**, *178*, 114305. [CrossRef]

10. Aalborg, H.A.; Molnár, P.; de Vries, J.E. What can explain the price, volatility and trading volume of Bitcoin? *Financ. Res. Lett.* **2019**, *29*, 255–265. [CrossRef]

11. Bovet, A.; Campajola, C.; Mottes, F.; Restocchi, V.; Vallarano, N.,; Squartini, T.; Tessone, C.J. The evolving liaisons between the transaction networks of Bitcoin and its price dynamics. *Proc. Blockchain Kaigi 2022* **2023**, *40*, 011002.

12. Peterson, T. To the Moon: A History of Bitcoin Price Manipulation. *J. Forensic Investig. Account.* **2021**, *13*, 254–272. [CrossRef]

13. M'bakob, G.B. Bubbles in Bitcoin and Ethereum: The role of halving in the formation of super cycles. *Sustain. Futur.* **2024**, *7*, 100178. [CrossRef]

14. Koki, C.; Meligkotsidou, L.; Vrontos, I. Forecasting under model uncertainty: Non-homogeneous hidden Markov models with Pòlya-Gamma data augmentation. *J. Forecast.* **2020**, *39*, 580–598. [CrossRef]

15. Koki, C.; Leonardos, S.; Piliouras, G. Do Cryptocurrency Prices Camouflage Latent Economic Effects? A Bayesian Hidden Markov Approach. *Future Internet* **2021**, *12*, 59. [CrossRef]

16. Chen, Y. Empirical analysis of bitcoin price. *J. Econ. Financ.* **2021**, *45*, 692–715. [CrossRef]

17. Katsiampa, P. An Empirical Investigation of Volatility Dynamics in the Cryptocurrency Market. *Res. Int. Bus. Financ.* **2019**, *50*, 322–335. [CrossRef]

18. Tiwari, A.K.; Jana, R.K.; Das, D.; Roubaud, D. Informational Efficiency of Bitcoin—An Extension. *Econ. Lett.* **2019**, *191*, 108735. [CrossRef]

19. Kodama, O.; Pichl, L.; Kaizoji, T. Regime Change And Trend Prediction For Bitcoin Time Series Data. *CBU Int. Conf. Proc.* **2017**, *5*, 384–388. [CrossRef]

20. Alam, N.; Dutta, A. Interdependence of Bitcoin and Conventional Currencies under Different Regime Structures. *Financ. Res. Lett.* **2021**, *38*, 101439.

21. Bouri, E.; Jain, A.; Roubaud, D.; Kristoufek, L. Cryptocurrencies as an Asset Class? An Empirical Assessment through the Lens of a New Regime-Switching Approach. *J. Int. Financ. Mark. Inst. Money* **2021**, *74*, 101451.

22. George, E.; McCulloch, R. Approaches for Bayesian Variable Selection. *Stat. Sin.* **1997**, *7*, 339–373.

23. Polson, N.G.; Scott, J.G.; Windle, J. Bayesian inference for logistic models using Pólya–Gamma latent variables. *J. Am. Stat. Assoc.* **2013**, *108*, 1339–1349. [CrossRef]

24. Box, G.E.P.; Jenkins, G.M. *Time Series Analysis: Forecasting and Control*; John Wiley & Sons: Hoboken, NJ, USA, 2015.

25. Efron, B. Bootstrap Methods: Another Look at the Jackknife. *Ann. Stat.* **1979**, *7*, 1–26. [CrossRef]

26. Gelman, A.; Rubin, D.B. Inference from Iterative Simulation Using Multiple Sequences. *Stat. Sci.* **1992**, *7*, 457–-472. [CrossRef]

27. Wang, J.,; Ma, F.; Bouri, E.; Guo, Y. Which factors drive Bitcoin volatility: Macroeconomic, technical, or both? *J. Forecast.* **2023**, *42*, 970–988. [CrossRef]

28. Ibrahim, A.; Kashef, R.; Li, M.; Valencia, E.; Huang, E. Bitcoin Network Mechanics: Forecasting the BTC Closing Price Using Vector Auto-Regression Models Based on Endogenous and Exogenous Feature Variables. *J. Risk Financ. Manag.* **2020**, *13*, 189. [CrossRef]

29. Perepelitsa, M. Elementary Bitcoin economics: From production and transaction demand to values. *arXiv* **2022**, arXiv:2211.07035.

30. Basher, S.A.; Sadorsky, P. Forecasting Bitcoin price direction with random forests: How important are interest rates, inflation, and market volatility? *Mach. Learn. Appl.* **2022**, *9*, 100355.

31. Wang, L.; Sarker, P.K.; Bouri, E. Short- and Long-Term Interactions Between Bitcoin and Economic Variables: Evidence from the US. *Comput. Econ.* **2023**, *61*, 1305–1330. [CrossRef]

32. Katsiampa, P. Volatility estimation for Bitcoin: A comparison of GARCH models. *Econ. Lett.* **2017**, *158*, 3–6. [CrossRef]

33. Bouri, E.; Azzi, G.; Dyhrberg, A.H. On the return-volatility relationship in the Bitcoin market around the price crash of 2013. *Economics* **2017**, *11*, 2. [CrossRef]

34. Makridakis, S.; Andersen, A.; Carbone, R.; Fildes, R.; Hibon, M.; Lewandowski, R.; Newton, J.; Parzen, E.; Winkler, R. The accuracy of extrapolation (time series) methods: Results of a forecasting competition. *J. Forecast.* **1982**, *1*, 111–153. [CrossRef]

35. Politis, D.N.; Romano, J.P. The stationary bootstrap. *J. Am. Stat. Assoc.* **1994**, *89*, 1303–1313. [CrossRef]

36. Wątorek, M.; Kwapień, J.; Drożdż, S. Cryptocurrencies Are Becoming Part of the World Global Financial Market. *Entropy* **2023**, *25*, 377. [CrossRef]
37. Kaiser, B.; Jurado, M.; Ledger, A. The looming threat of China: An analysis of chinese influence on Bitcoin. *arXiv* **2018**, arXiv:1810.02466.
38. Meligkotsidou, L.; Dellaportas, P. Forecasting with non-homogeneous hidden Markov models. *Stat. Comput.* **2011**, *21*, 439–449. [CrossRef]